

## Enhanced Paracetamol Oxidation and Its Determination using Electrochemically Activated Glassy Carbon Electrode

Mohamed I. Awad<sup>1,2,\*</sup>, Ali Sayqal<sup>1</sup>, Rami Adel Pashameah<sup>1</sup>, Ahmed M. Hameed<sup>1</sup>, Moataz Morad<sup>1</sup>, Hussain Alessa<sup>1</sup>, Reem Kamal Shah<sup>1</sup>, Mohammed. A. Kassem<sup>1,2,\*</sup>

<sup>1</sup> Chemistry Department, Faculty of Applied Science, Umm Al-Qura University, Makkah, Saudi Arabia.

<sup>2</sup> Chemistry Department, Faculty of Science, Cairo University, Cairo, Egypt

<sup>3</sup> Chemistry Department, Faculty of Science, Benha University, Benha13518, Egypt

\*E-mail: [miawad@uqu.edu.sa](mailto:miawad@uqu.edu.sa) & [mawad70@yahoo.com](mailto:mawad70@yahoo.com), [maa\\_kassem@hotmail.com](mailto:maa_kassem@hotmail.com) & [makassem@uqu.edu.sa](mailto:makassem@uqu.edu.sa)

Received: 25 August 2020 / Accepted: 11 October 2020 / Published: 30 November 2020

---

Herein, the impact of electroactivation of glassy carbon electrode on the paracetamol drug electrochemical behavior is investigated for the first time. The morphology of the GC electrode surface was investigated using SEM. The extent of oxidation of GC as well as the pH of the supporting electrolyte has been investigated. The oxidation of GC results in the formation of several containing oxygen functional groups which increases with increasing the number of potential cycles for oxidation. The extent of GC oxidation was quantified by calculating the number of surface's quinone units (S), as calculated from the voltammetric measurements in 1.0 M H<sub>2</sub>SO<sub>4</sub>. Then the S was correlated with the extent of electrocatalytic oxidation of PC. Based on the voltammetric studies, it has been found that the oxidation of PC is controlled by both diffusion and adsorption processes. Finally, the activation of GC electrode was used for the quantitative determination of PC in a suitable rectilinear range with a standard deviation and relative standard deviation (RSD) of 0.17 mM and 2.4%, respectively.

---

**Keywords:** Oxidized glassy carbon; Paracetamol; Cyclic voltammetry; Electrocatalysis; Analytical determination.

### 1. INTRODUCTION

Paracetamol (p-hydroxy acetanilide or *N*-acetyl-*p*-aminophenol, PC) of chemical structure shown in Fig. 1, is one of analgesic and antipyretic compound commonly used for fever and headache relief in addition to several applications in pharmaceutical industries. It can be used as an alternative to aspirin for some patients who cannot tolerate aspirin. Overdoses are associated with hepatotoxicity and can cause organ failure within short time, so it be used in the safe dose. It is believed that the main source

of danger of acetaminophen is its metabolite whereas it is considered as actual hepatotoxic agent [1-9]. Accumulation of toxic metabolites often accompany overdose of PC, and a severe hepatotoxicity and nephrotoxicity occur. Thus, for the sake of quality assurance of pharmaceutical industry and related industries, estimation of PC is vital for the healthcare industry [10-12]. Several methods have been reported for the estimation of PC in drug formulations. It includes, for instance, spectrophotometry [13-15], reverse phase high performance liquid chromatography [16-24], capillary electrophoresis [25-27] and chemiluminescence [28-30]. Some of these methods are tedious as they require several preliminary steps before the determination, and some is time-consuming. In general, these methods are not suitable for the routine analysis of PC as they require expensive instruments or the need of sample pre-treatment steps for analysis. Thus, simpler procedures performed in relatively shorter times without using numerous chemicals are preferable. Electrochemical methods found their way for analysis of paracetamol specially at modified electrodes which introduce the selectivity as well as the sensitivity [31-35]. PC is electrochemically active, and its response has been reported on various types of electrodes, both solid, bare and modified as well as mercury electrode [36-40]. However, the behavior at electrochemically activated glassy carbon (EAGC) electrode has not been reported, even though glassy carbon electrode is the first choice for such species as it is characterized by wide potential range as well as the simple control of the surface and the possible derivatization with functional groups. The present study aims at the enhancement of PC oxidation in aqueous solutions using EAGC, and the subsequent application for PC quantification. The extent of oxidation of GC as well as the pH of the supporting electrolyte has been investigated.

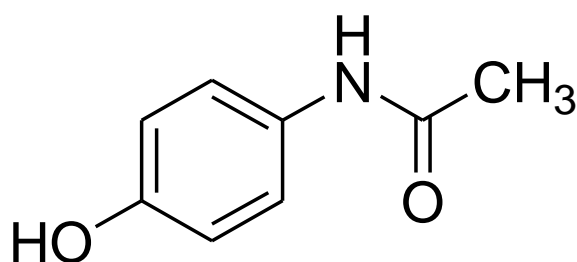


**Figure 1.** The structure of paracetamol (PC)

## 2. EXPERIMENTAL

### 2.1. Materials and Reagents:

Chemicals used were of analytical grade and were used as received. Sulfuric acid (H<sub>2</sub>SO<sub>4</sub>, Omni Trace Ultra) was purchased from Sigma-Aldrich. Sodium hydroxide (NaOH, 99.8% purity) was purchased from BDH. Phosphate buffer solutions of different pHs were prepared using NaH<sub>2</sub>PO<sub>4</sub>/Na<sub>2</sub>HPO<sub>4</sub> couples according to the reported method [41]. A pure powder of paracetamol (PC) was gifted from Amriya Pharmaceutical Industries, Egypt. A freshly stock solution of suitable

concentration of PC was prepared by dissolving a suitable amount of the powder in bi-distilled water. Prior to electrochemical measurements, electrolyte solutions were de-aerated by N<sub>2</sub>-bubbling.

## 2.2. Glassy carbon electrodes electroactivation:

The GC electrode (3 mm diameter) was mechanically polished with fine alumina powder and then rinsed with water before sonication process to remove physically adsorbed species. Then, GC was either used directly or after being electro-activated. The activation process was optimized by cycling of potential in the potential range -0.2 to 2 V for suitable number of potential cycles. The anodic oxidation of GC in H<sub>2</sub>SO<sub>4</sub> increase the percentage of functional groups bearing –OH group onto the electrode surface. The electrode after oxidation was assigned as GCox.

## 2.3. Measurements:

Electrochemical measurements were performed using a PGSTAT30 potentiostat/galvanostat (Netherlands) controlled by General Purpose Electrochemical Systems (GPES) and Frequency Response Analyzer (FRA) software. A conventional three-electrode cell of around 20 ml and equipped with Ag/AgCl (KCl sat.) reference electrode and Pt spiral wire auxiliary electrode was used for the cyclic voltammetric measurements. All electrochemical measurements were conducted under nitrogen saturated solutions. SEM was taken using a Hitachi microscope of accelerating voltage of 20 kV.

## 3. RESULTS AND DISCUSSION

SEM images of bare and oxidized glassy carbon electrodes are shown in Fig. 2. GC was oxidized by applying 5 potential cycles in 0.5 M H<sub>2</sub>SO<sub>4</sub> as mentioned in the experimental section. As shown in the figure, the roughness of the oxidized electrode is significant (image b) compared with the bare GC electrode of smooth surface (image a). It has been reported that roughness could be used as indication of the extent of oxidation of the GC electrode, increasing the extent of oxidation increases the roughness of GC[42]. The oxidation of GC electrode results in the formation of several oxygen-containing functional groups that changes the surface properties of the thus oxidized electrode [37].

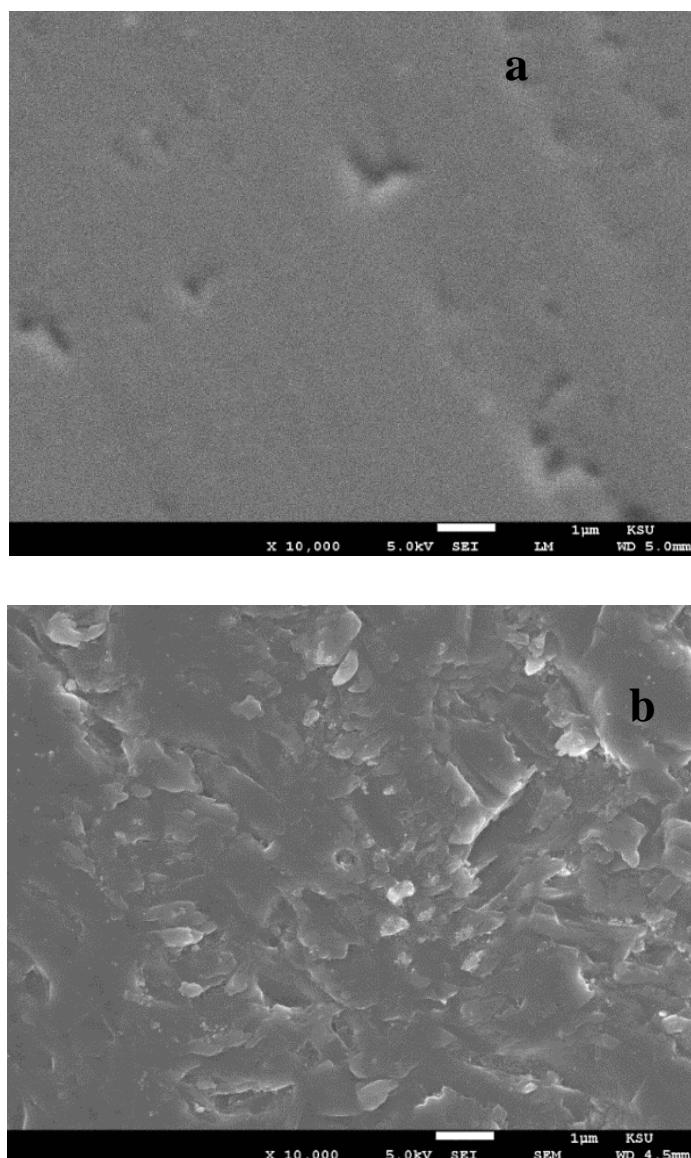


**Figure 2.** SEM images for (a) bare GC and (b) GCox electrodes. GC was oxidized by applying 5 potential cycles in 0.5 M  $\text{H}_2\text{SO}_4$  with scan rate 100 mV/s.

### 3.1. The electrochemical behavior of PC on activated GC

Fig. 3 shows cyclic voltammograms obtained at (a) bare and (b-e) electrochemically pretreated GC in PB containing 12.5 mM PC. GC was oxidized as mentioned in the experimental section. Parameters extracted from this figure are given in Table 1. Interestingly, the response of PC obtained at bare GC is significantly changed at the oxidized GC; the anodic peak is obtained at relatively large potential (curve a) compared with that obtained at the electrochemically pretreated one (curves b-e) and the cathodic one at ca. 0.2 V is ill defined as previously reported [43]. At the oxidized GC, the well anodic peak coupled with the well-defined cathodic one is revealed. The extent of catalysis is dependent on the extent of oxidation of the GC electrode; when the electrode is subjected to one potential cycles for activation the response of PC is significantly changed, and the  $\Delta E = 85$  mV is obtained. Upon

increasing the number of potential cycles for oxidation of GC electrode, the behavior does not change significantly with respect to  $\Delta E = 85$  mV.

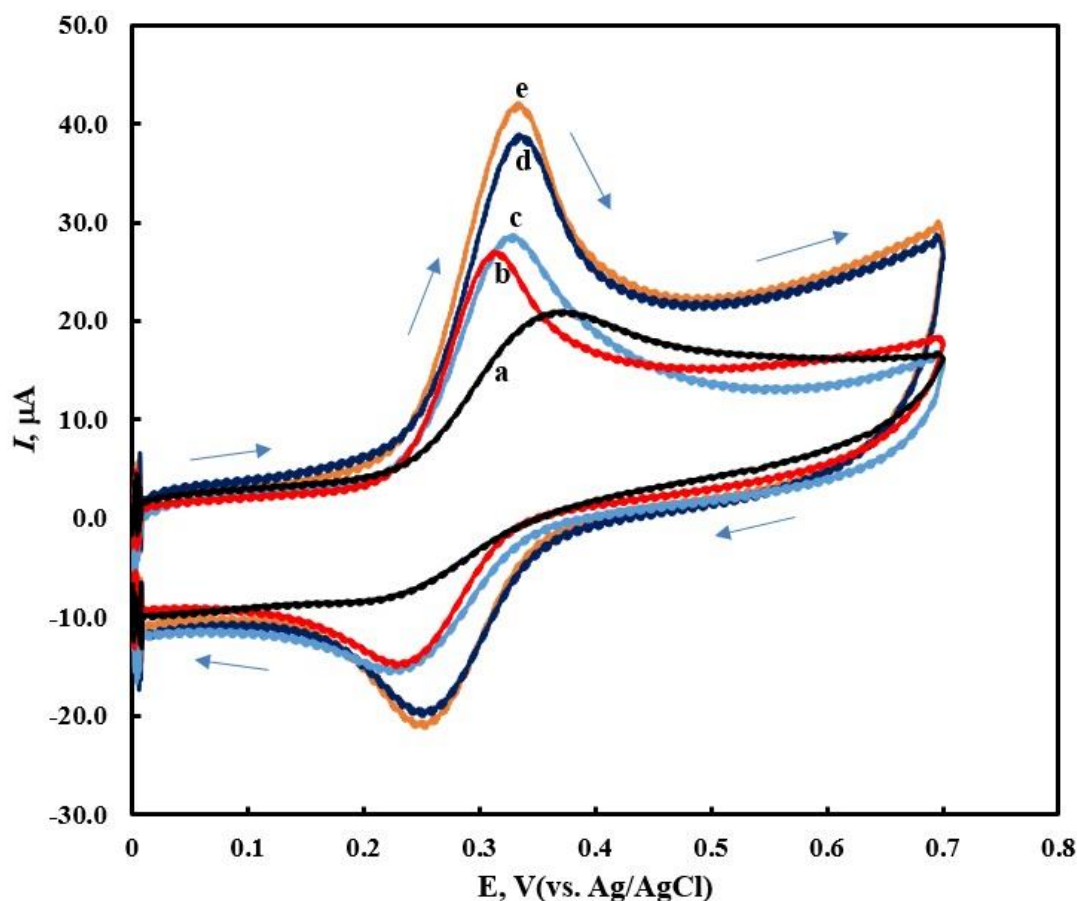


**Figure 3.** CVs obtained at a) bare and (b-d) oxidized GC in PB (pH 7) containing 12.5 mM PC. Number of cycles used for oxidation of GC was b) one, c) three, d) five and e) six cycles. Scan rate = 100 mV/sec.

However, the current response for the oxidation and reduction continue in increasing. This points to the increase in the surface area of the electrode. A point which is useful for the sake of analysis of PC. It seems that the oxidation of GC results in the formation of several oxygen-contained functional groups upon the first cycles and with increasing the number of cycles, the roughness increases resulting in increasing the surface area as represented above in the SEM images. Under the studied pH range, PC is oxidized to N-acetyl-p-quinoneimine in an electrochemical step involving two electrons and two protons to produce N-acetyl-p-quinoneimine. This step is followed by non-electrochemical reaction steps which are pH dependent. In strongly acidic media, PC is oxidized finally to benzoquinone [43-45] according to the following mechanism:

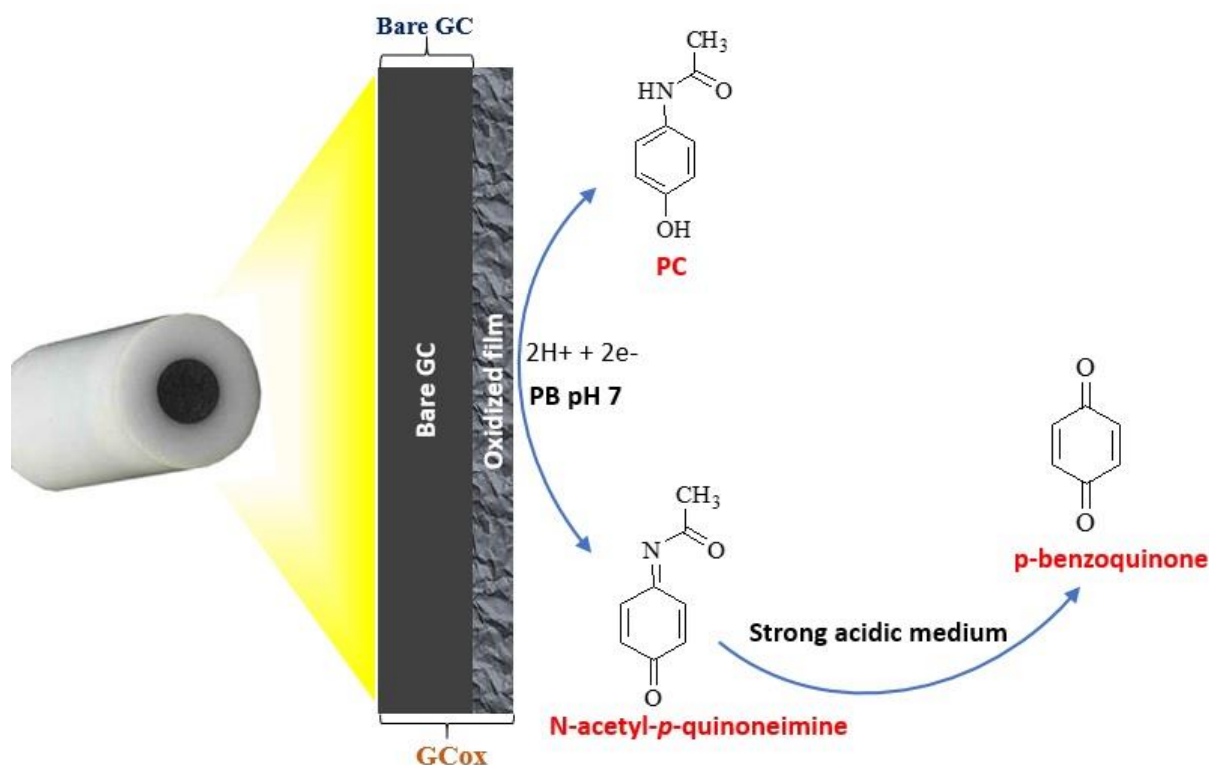


**Figure 4.** The proposed mechanism for oxidation of PC at GCox

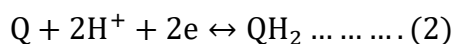
**Table 1.** Electrochemical parameters for oxidation of PC at GC and GCox in PB at scan rate 100 mV/s

Electrodes	$I_{pa}$ ( $\mu$ A)	$I_{pc}$ ( $\mu$ A)	$E_{pa}$ (mV)	$E_{pc}$ (mV)	$\Delta E$ (mV)
Bare GC	14.5	6.1	365	200	165
GCox (one cycle)	22.0	13.1	320	235	85
GCox (3 cycles)	24.3	13.6	340	235	105
GCox (5 cycles)	31.3	15.9	335	250	85
GCox (6 cycles)	34.1	17.0	335	250	85

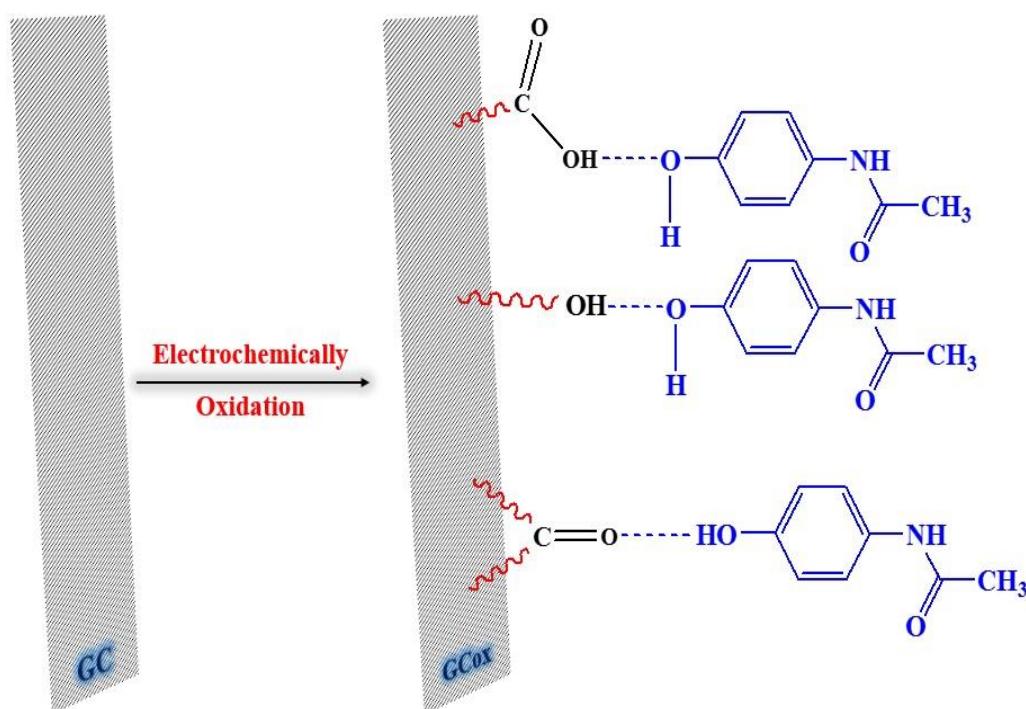
The enhancement of the PC electrochemical behavior is thought to be related to the quinone (Q) functional groups formed upon oxidation of GC. It has been reported that quinone functional groups to enhance the oxygen reduction [46]. However, in the present case the confined quinone redox couple appears at much lower positive potential compared with the electrooxidation peak of PC. Thus, the possible reason for activation of PC oxidation is the enhancement of interaction of PC with the generated functional group on the GC surface, possibly by hydrogen bond. Similar behavior reported that adsorbed quinone mediates some reactions. However, for the same reaction the Q groups generated electrochemically did not mediate it [47,48]. The increase in enhancement upon increasing the extent of oxidation is related to the number of surface quinone units, calculated by the following equation;

$$S = \frac{NC}{nF} \dots \dots (1)$$

where  $N$  is the Avogadro number,  $n$  is the number of electrons included in the following equation:



and  $F$  is the Faraday constant.  $C$  is the charge obtained by the integration of the CV of the (Q/QH<sub>2</sub>) redox couple obtained for the oxidized GC in 1 M H<sub>2</sub>SO<sub>4</sub> (data are not shown). The number of active sites for GC oxidized by one, three, five and six cycles equals  $7.0 \times 10^{14}$ ,  $9.3 \times 10^{14}$ ,  $2.1 \times 10^{16}$  and  $2.7 \times 10^{16}$ , respectively. The relation between  $\log S$  and the anodic peak current for paracetamol is given in Fig. 5. It is clearly shown that the peak current is related to the number of surface's quinone units. It becomes clear that electrooxidation of GC critically catalyzes the oxidation of PC via the generation of functional groups which enhances the interaction of PC with such generated groups, as represented in the following scheme;



**Scheme 1.** The proposed interaction between PC and the generated functional groups on GCox



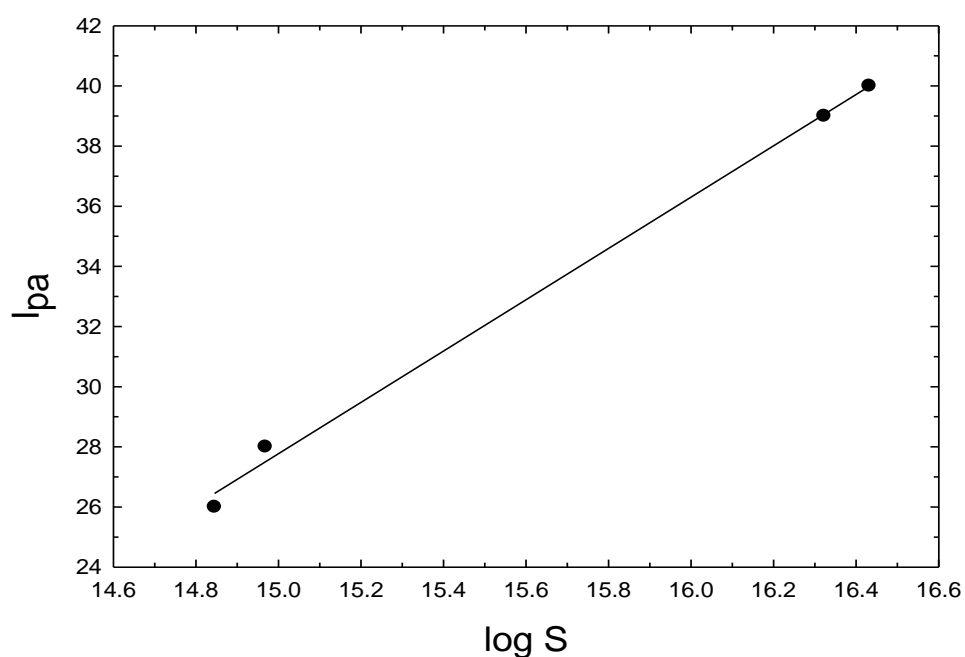


**Figure 5.** The relation between  $\log S$  and the anodic peak current for PC. The number of surface's quinone units ( $S$ ) was estimated using equation 1.

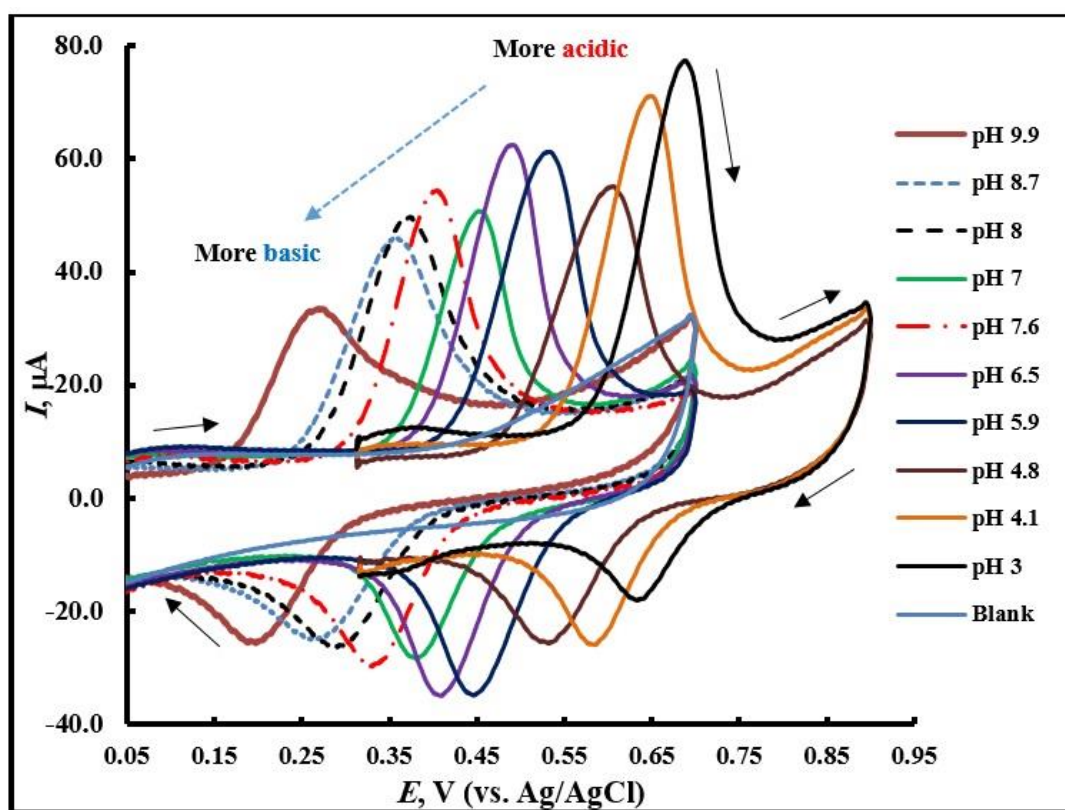


**Figure 6.** Effect of pH on the voltammetric behaviour of 12.5 mM PC at GCox. GC was oxidized by applying 5 potential cycles in 0.5 M  $H_2SO_4$  with scan rate 100 mV/s.

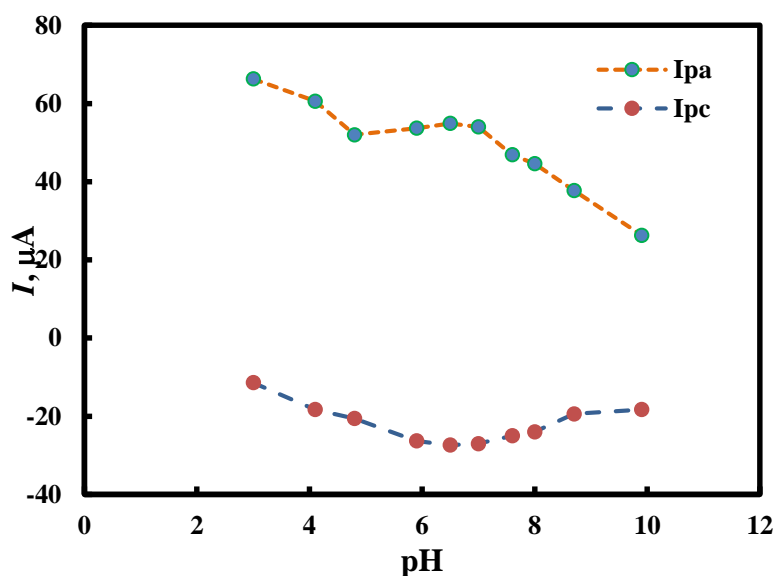


### 3.2. The influence of pH on the electrochemical behavior of PC on activated GC

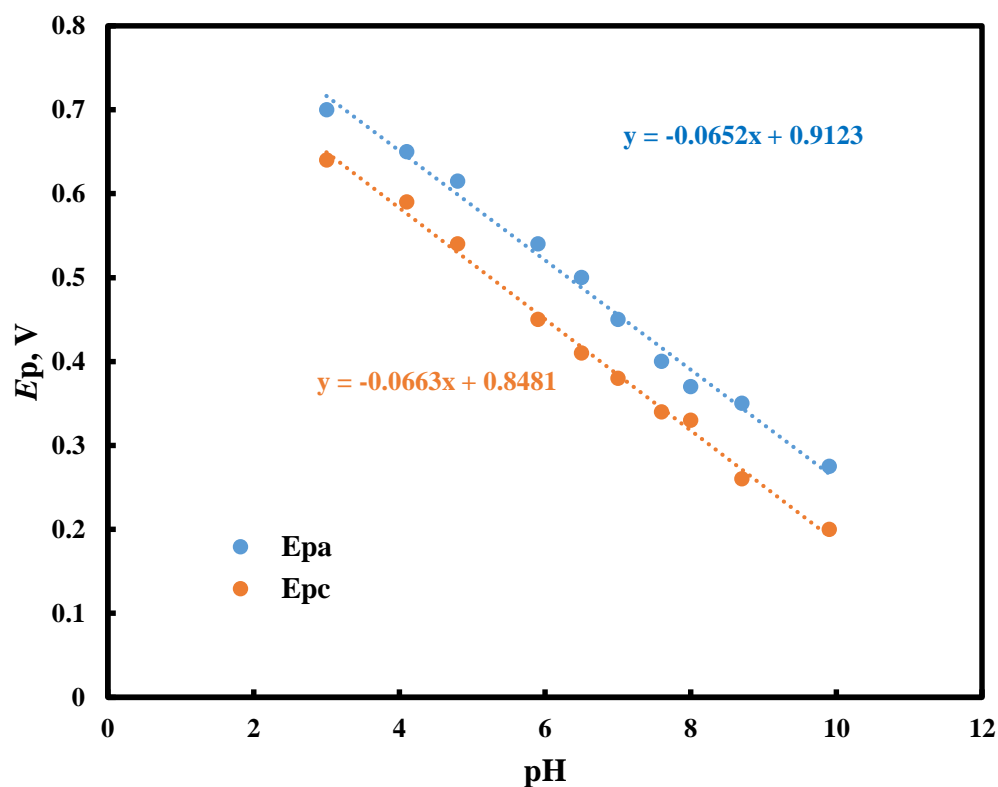
The pH of the supporting electrolyte for reaction containing protons as a reactant or product is critical in electroanalysis as the pH largely affects the electrode–solution interface, and consequently the kinetics of the charge transfer process. The pH dependence of PC oxidation at GCox is shown in Fig. 6 and Table 2. Within the studied pH range, the redox couple is obtained with a negative shift as expected upon increasing the pH. The peak current for the anodic ( $I_{pa}$ ) and cathodic ( $I_{pc}$ ) peaks as well as their peak potentials are plotted against pH and shown as Figs. 7 and 8, respectively. In Fig. 7, it is obvious that, the effect on the anodic peak current is larger compared with that of the cathodic one.  $I_{pc}$  decreases regularly with increasing the pH, while the dependence of  $I_{pc}$  on the pH is not regular. Regarding the effect on the peak potential, parallel straight lines for both peaks are obtained. At pH 7, an acceptable response is obtained, and thus it was chosen for the following measurements. Linear relationships of the peak potential of PC as a function of pH following Nernst's equation;

$$E_p = E_{\text{formal}}^o - \frac{2.3RTm}{nF} \text{pH} \dots \dots (3)$$

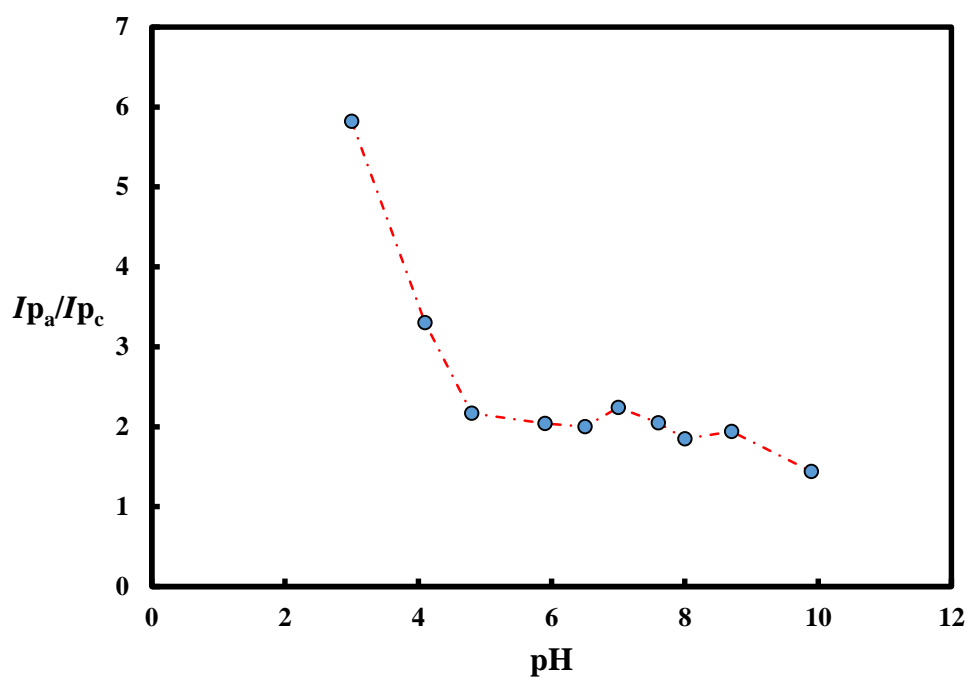
where  $m$  and  $n$  represent the number of protons and electrons, respectively. Slopes around 60 mV per pH is obtained for both peaks indicating Nernstian behaviour. This indicates that PC oxidation is accompanied by the transfer of ( $2e^-/2H^+$ ), i.e., equal number of protons and electrons [49]. It has been reported that PC oxidation and the oxidation product is pH dependant. It is noteworthy to mention the large dependence of  $I_{pa}/I_{pc}$  on the pH (shown in Fig. 9); it changes from around 1.4 at pH 9.9 to 5.8 at pH 3. This points to the increase in the reversibility with decreasing pH as reflected on the significant change in the values of the difference in peak potential between anodic and cathodic peaks ( $\Delta E$ ); it equals 80 mV at pH 9.9 and 60 mV at pH 3.



**Figure 7.** Relation between pH and peak currents for 12.5 mM PC at GCox activated by five oxidation cycles. Data were extracted from Fig 6.



**Figure 8.** Relation between pH and peak potentials for 12.5 mM PC at GCox activated by five oxidation cycles. Data were extracted from Fig 6.

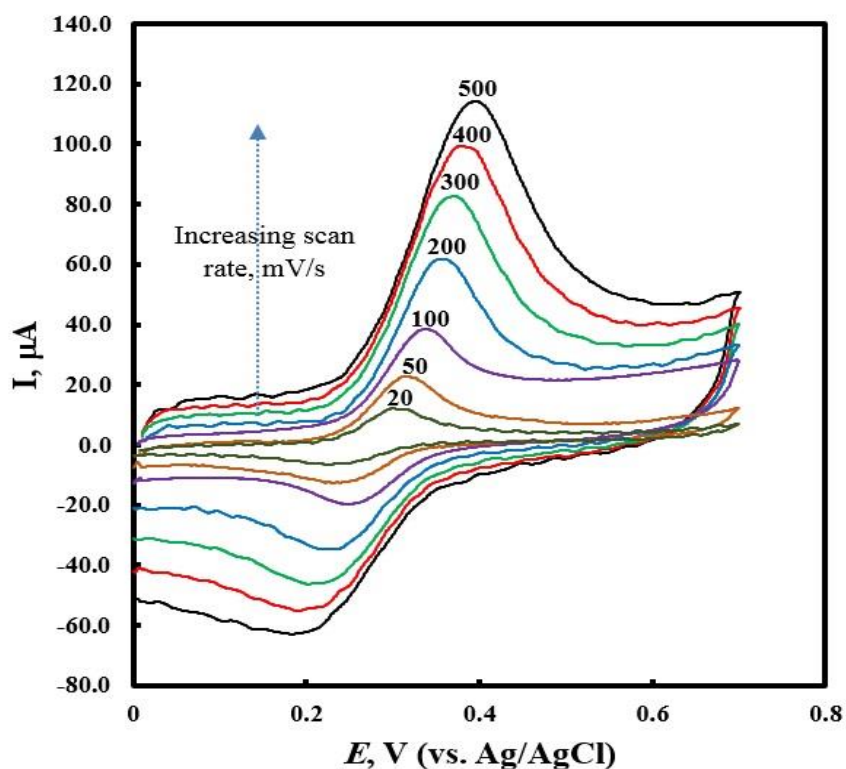


**Figure 9.** Relation between pH and  $I_{pa}/I_{pc}$  for 12.5 mM PC on GCox after five oxidation cycles. Data were extracted from Fig 6.

**Table 2.** Relation between pH and peak potentials and peak currents for electrochemical behavior of PC on GCox at scan rate 100 mV/s

pH	$I_{pa}$	$I_{pc}$	$E_{pa}$	$E_{pc}$	$E_{pa}-E_{pc}$	$I_{pa}/I_{pc}$	$\log(I_{pa}/I_{pc})$
3.0	66.3	11.4	0.7	0.64	60	5.82	0.76
4.1	60.6	18.3	0.65	0.59	60	3.3	0.52
4.8	44.6	20.6	0.615	0.54	75	2.17	0.34
5.9	53.7	26.3	0.54	0.45	90	2.04	0.31
6.5	54.9	27.4	0.5	0.41	90	2	0.3
7.0	43.4	19.4	0.45	0.38	70	2.24	0.35
7.6	46.9	22.9	0.4	0.34	60	2.05	0.31
8.0	44.6	24	0.37	0.33	40	1.85	0.27
8.7	37.7	19.4	0.35	0.26	90	1.94	0.29
9.9	26.3	18.3	0.275	0.2	75	1.44	0.16

### 3.3. Scan rate dependence

**Figure 10.** CVs obtained at EAGC electrode in PB (pH 7) containing 12.5 mM PC at various scan rates (Numbers of scan rates are in mV/s). GC was oxidized by applying 5 potential cycles in 0.5 M  $H_2SO_4$  with scan rate 100 mV/s.

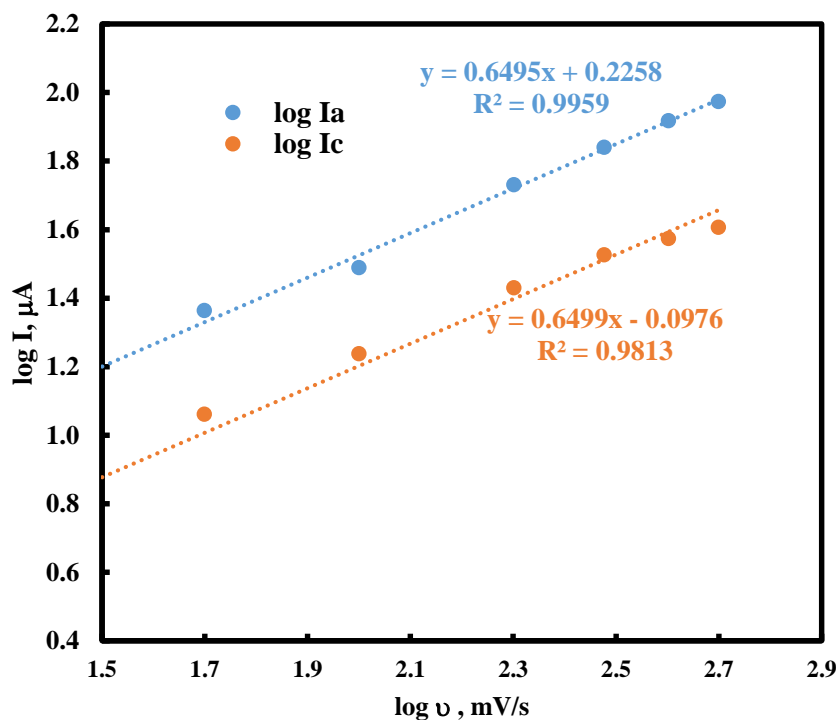


**Figure 11.** Relation between log scan rate and log peak current. Data were taken from Figure 10.

The effect of scan rate on the peak current and peak potential is utilized in evaluating the type of mass transport process as well as the electrode kinetics for a certain reaction. Fig. 10 shows the effect of scan rate on CVs of the oxidation of PC at GCox electrode. As clearly shown, anodic and cathodic peaks are shifted with increasing the scan rate pointing that the process is not reversible one. The log-log plot for  $I_{pa}$  and scan rate is shown in Fig. 11. The peak current dependence on scan rate is linear. The linear regression equation was  $y = 0.6495x + 0.2258$  with a correction coefficient of 0.9959. Based on the obtained equation, a slope of 0.6495 reveals that the process is controlled by both diffusion and adsorption processes with the former is the predominant.

### 3.4 Electroanalytical determination of PC using the oxidized GC

Under the above optimum EAGC electrode, Fig. 12 represented the calibration curve for the determination of PC (inset, the linear sweep voltammetry (LSV) for the determination of PC at different concentrations). The linear dynamic range for the determination of PC was found to be 3.0-6.5 mM with a good correlation coefficient  $R^2 = 0.9979$ . To measure the precision of the developed method, both standard deviation and relative standard deviation (RSD) for five measurements for 7.0 mM PC were calculated and found to be 0.17 mM and 2.4%, respectively. The regression equation for this method is as the following:

$$I(\mu A) = 11.169 [PC](mM) - 5.6525 \dots\dots(4)$$

To test the validity of the proposed method and its significance, F-test was performed by comparing the variance of our method with that of reference one [31], at 95% confidence level. Results as seen in Table 3 indicated that results obtained by the present methods are significant.

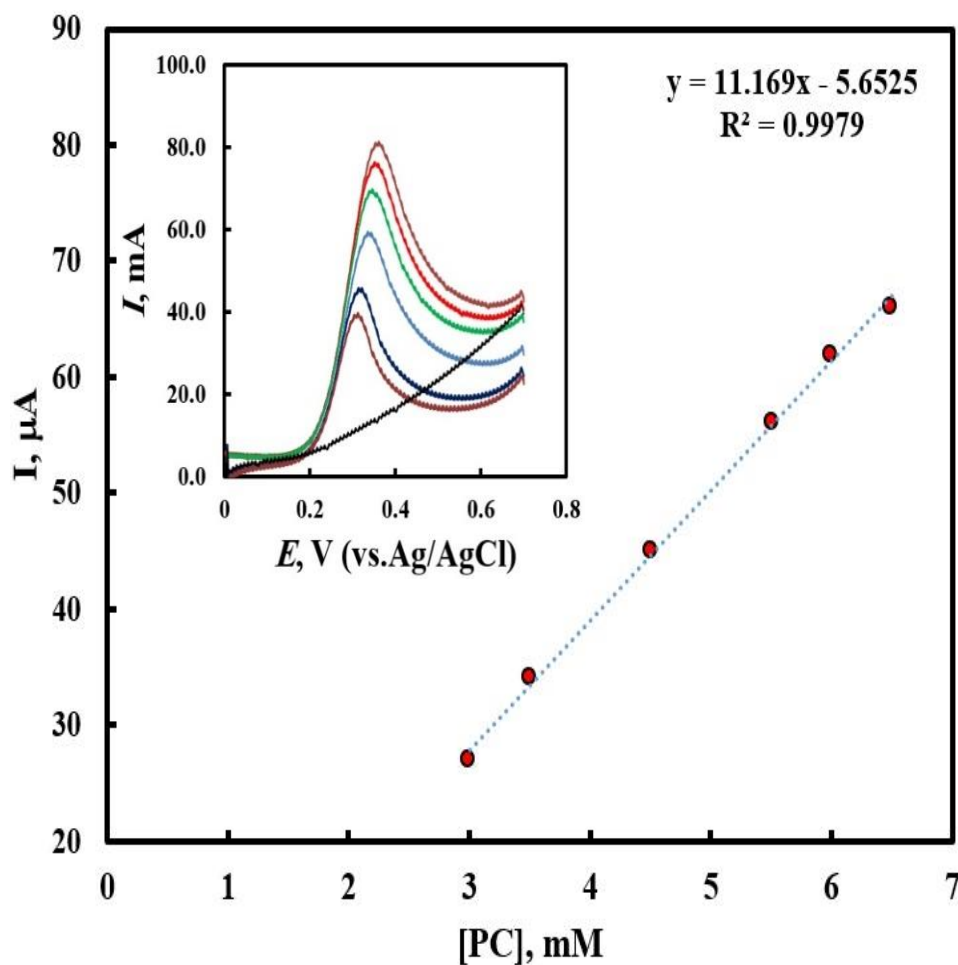


**Figure 12.** Calibration curve for determination of PC using EAGC. (Inset, the linear sweep voltammetry). GC was oxidized by applying 5 potential cycles in 0.5 M H<sub>2</sub>SO<sub>4</sub> with scan rate 100 mV/s.

**Table 3.** Parameters for the electrochemical determination of PC by GCox electrode using LSV.

Parameters	PC
Type of buffer	Phosphate
pH	7.0
Potential of measurement, V	0.3-0.35
Scan rate, mV/s	100
Linear concentration range, mM	3.0-6.5
<i>Regression equation<sup>a</sup></i>	
Slope, μA/mM	11.169
Intercept, μA	-5.6525

Correlation coefficient, $R^2$	0.9979
Standard deviation, SD (n=5), mM	0.17
Relative Standard deviation, RSD <sup>b</sup> , %	2.4
LOD, mM	0.281
LOQ, mM	0.842
SD of slope	0.19
SD of intercept	0.95
F-test <sup>c</sup>	3.11

<sup>a</sup>  $I(\mu\text{A}) = \text{slope [PC]}(\text{mM}) \pm \text{Intercept}$

<sup>b</sup> Average of five consecutive measurements.

<sup>c</sup> The theoretical value for F at n = (8,5) at 95% confidence level is 6.09

#### 4. CONCLUSIONS

Using EAGC electrode, paracetamol oxidation was significantly enhanced. The electrooxidation of GC electrode in 0.5 M H<sub>2</sub>SO<sub>4</sub> changed the electrode surface by the formation of several oxygen-containing functional groups that changes the surface properties of the thus oxidized electrode. The electrooxidation of PC using this electrode was found to be controlled by both diffusion and adsorption processes. A correlation of the electroactivity of EAGC electrode with the number of generated quinone sites is figured. Next, EAGC was successfully used for the determination of PC.

#### ACKNOWLEDGEMENT

The Authors would like to thank the Deanship of Scientific Research at Umm Al-Qura University for supporting this work by Grant Code: 19-SCI-1-01-0004

#### References

1. C.M. Kuskur, K.B. Swamy and H. Jayadevappa, *Ionics*, 25 (2019) 1845.
2. N. Wangfuengkanagul and O. Chailapakul, *J. Pharm. Biomed. Anal.*, 28 (2002) 841.
3. P.I. Dargan and A.L. Jones, *Drug Saf.*, 25 (2002) 625.
4. Y. Nademi, S.A. Iranagh, A. Yousefpour, S.Z. Mousavi and H. Modarress *J Chem Sci*, 126 (2014) 637.
5. J.G. O'Grady, G.J.M. Alexander and K.M. Hayllar, *Gastroenterology*, 97 (1989) 439.
6. J.A. Vale and A.T. Proudfoot, *Lancet*, 346 (1995) 547.
7. D.C. Dahlin, G.T. Miwa, A.Y.H. Lu and S.D. Nelson, *Proc. Natl. Acad. Sci.*, 81 (1984) 1327.
8. H. Dong, R.L. Haining, K.E. Thummel, A.E. Rettie and S.D. Nelson, *Drug Metab. Dispos.*, 28 (2000) 1397.
9. Q. Wan, X. Wang, F. Yu, X. Wang and N. Yang, *J. Appl. Electrochem.*, 39 (2009) 785.
10. M.M. Soliman, M.A. Nassan and T.A. Ismail, *BMC Complementary Altern. Med.*, 14 (2014) 457.
11. W.J. Holubek, S. Kalman and R.S. Hoffman, *Hepatology*, 43 (2006) 880.
12. H. Jaeschke, C.D. Williams, A. Ramachandran and M.L. Bajt, *Liver Int.*, 32 (2012) 8.
13. N. Erk and F. Onour, *Anal. Lett.*, 30 (1997) 1201.
14. B.D.A. Elik and N. Altunay, *Microchem. J.*, 154 (2020) 104645.
15. S. Glavanović, M. Glavanović and V. Tomišić, *Spectrochim. Acta, Part A*, 15715 (2016) 258.

16. F. Canada-Canada, A. Espinosa-Mansilla, A.M. and de la Pena, *J. Sep. Sci.*, 30 (2007) 1242.
17. K. Srogi, *Anal. Lett.*, 39 (2006) 231.
18. İ.M. Palabıyık and F. Onur, *Chroma*, 66 (2007) 93.
19. S. Abbasi, S.A. Haeri and S. Sajjadifar, *Microchem. J.*, 146 (2019) 106.
20. M. Attimarad, *Pharm. Methods*, 2 (2011) 61.
21. E.A. Abdelaleem, I.A. Naguib, E.S. Hassan and N.W. Ali, *J. Pharm. Biomed. Anal.*, 11410 (2015) 22.
22. E.A. Abdelaleem and N.S. Abdelwahab, *Anal. Methods*, 5 (2013) 541.
23. I. Baranowska and B. Kowalski, *Water Air Soil Pollut.*, 211 (2010) 417.
24. G.M. Hadad, S. Emara and W.M. Mahmoud, *Talanta*, 79 (2009) 1360.
25. T. Perez-Ruiz, C. Martinez-Lozano, V. Tomas and R. Galera, *J. Pharm. Biomed. Anal.*, 38 (2005) 87.
26. A. Alnajjar, H.H. AbuSeada and A.M. Idris, *Talanta*, 72 (2007) 842.
27. S. Azhagvuel and R. Sekar, *J. Pharm. Biomed. Anal.*, 43 (2007) 873.
28. J. Lopez-Flores, M.L.F.D. Cordova and A. Molina-Diaz, *Anal. Chim. Acta*, 535 (2005) 161.
29. E. Wolyniec, U. Niedzwiedzka and A. Kojlo, *Instrum. Sci. Technol.*, 35 (2007) 219.
30. A. Waseem, M. Yaqoob and A. Nabi, *Talanta*, 71 (2007) 56.
31. M. Boopathi, M.S. Won and Y.B. Shim, *Anal. Chim. Acta*, 512 (2004) 191.
32. R.M. Carvalho, R.S. Freire, S. Rath and L.T. Kubota, *J. Pharm. Biomed. Anal.*, 34 (2004) 871.
33. C.L. Devi and S.S. Narayanan, *Ionics*, 25 (2019) 2323.
34. S.F. Wang, F. Xie and R.F. Hu, *Sens. Actuators B*, 123 (2007) 495.
35. R.N. Goyal and S.P. Singh, *Electrochim. Acta*, 51 (2006) 3008.
36. Z.A. Alothman, N. Bukhari, S.M. Wabaidur and S. Haider, *Sens. Actuators B*, 146 (2010) 314.
37. F.G. Bidkorbeh, S. Shahrokhian, A. Mohammadi and R. Dinarvand, *Electrochim. Acta*, 55 (2010) 2752.
38. N.F. Atta and M.F. El-Kady, *Talanta*, 79 (2009) 639.
39. F.S. Felix, C.M.A. Brett and L. Angnes, *J. Pharm. Biomed. Anal.*, 43 (2007) 1622.
40. E. Keskin and A.S. Ertürk, *Ionics* 24 (2018) 4043.
41. D.D. Perrin, B. Dempsey, *Buffers for pH and Metal Ion Control*, John Wiley & Sons, Inc, New York (1974) pp 138.
42. A. Dekanski, J. Stevanovic, R. Stevanovic, B.Z. Nikolic and V.M. Jovanovic, *Carbon*, 39 (2001) 1195.
43. D.J. Miner, J.R. Rice, R.M. Riggin and P.T. Kissinger, *Anal. Chem.*, 53 (1981) 2258.
44. P.T. Kissinger, D.A. Roston, J.J. Van Benschoten, J.Y. Lewis and W.R. Heineman, *J. Chem. Educ.*, 60 (1983) 772.
45. T. Skeika, M.F. de Faria, N. Nagata and C.A. Pessoa, *J. Braz. Chem. Soc.*, 19 (2008) 762.
46. M.G. Sullivan, R. Kotz and O. Haas, *J. Electrochem. Soc.*, 2000, 147 (2000) 308.
47. T. Nagoaka, T. Sakai, K. Ogura and T. Yoshino, *Anal. Chem.* 58 (1986) 1953 .
48. T. Nagoaka and T. Yoshino, *Anal. Chem.*, 58 (1986) 1037.
49. A.J. Bard, L.R. Faulkner, *Electrochemical Methods, Fundamentals and Applications*, 2<sup>nd</sup> ed.; John Wiley & Sons: New York, 2000.